Proceedings of CONF-CIAP 2026 Symposium: International Conference on Atomic Magnetometer and Applications
DOI: 10.54254/2753-8818/2026.HZ28276

Study of Long-range Two-particle Correlations in $\sqrt{s} = 200$ GeV $p + p$ Collisions UsingPythia

Yimiao Liu

LieWu High School, Chengdu, China
liuyimiao21@gmail.com

Abstract. This study investigates long-range two-particle correlations in $\sqrt{s} = 200$~GeV proton-proton (p+p) collisions using Monte Carlo simulations with Pythia~8.315 (Monash 2013 tune). We systematically analyze charged particle correlations within $|\eta| < 1.1$ across various p_T ranges and multiplicity bins. A key finding for the low p_T region ($0.2 < p_T < 1.0$ ~GeV/ c) is the consistent flatness of two-particle correlation functions and the near-zero values of anisotropic flow coefficients (v_2, v_3), typically less than 0.005 , across all multiplicities and pseudorapidity gaps. This confirms the substantial suppression of jet contributions in this kinematic domain and establishes a crucial ``null'' non-flow baseline for identifying genuine collective flow signals in experimental data. Conversely, in the higher $p_T$ region ( $1.0 < p_T < 3.0$ ~GeV/ $c$ ), we observe prominent jet-like correlations. The $v_2$ coefficient exhibits a characteristic ``hill-like'' multiplicity dependence, which, along with $v_3 \ll v_2$, is attributed to the complex interplay of Multiple Parton Interactions (MPI) and Underlying Event (UE) contributions, extending over large pseudorapidity differences. OurPythiaresults, particularly the absence of a pronounced long-range ``ridge'' structure, align with preliminary sPHENIX Silicon Tracklet experimental data. This work provides a robust non-flow baseline for ongoing experimental searches for collective phenomena in small collision systems, elucidating the intricate contributions of standard QCD processes.

Keywords: Long-range correlations, Two-particle correlations,Proton-proton collisions, PYTHIA, RHIC

1. Introduction

The study of strongly interacting matter under extreme conditions, primarily through relativistic heavy-ion collisions, provides compelling evidence for the formation of a Quark-Gluon Plasma (QGP), a deconfined state of quarks and gluons [1]. A key signature of QGP formation is the observation of ``collective flow,'' manifest as long-range angular correlations among particles, which can be described by anisotropic flow coefficients (v_n). These collective phenomena were historically believed to be exclusive to large collision systems.

However, recent experimental discoveries of collective-like signatures in seemingly small collision systems like high-multiplicity proton-proton (p+p) [2,3] and proton-nucleus (p+A) collisions at RHIC and LHC energies challenge this conventional understanding. Two primary

© 2025 The Authors. This is an open access article distributed under the terms of the Creative Commons Attribution License 4.0 (https://creativecommons.org/licenses/by/4.0/).

DOI: 10.54254/2753-8818/2026.HZ28276

interpretations emerge: one attributes these phenomena to hydrodynamic effects in small systems, while the other suggests non-flow mechanisms, such as Multi-Parton Interactions (MPI), initial-state fluctuations, and various Underlying Event (UE) dynamics, are sufficient to explain the observed correlations [4].

To distinguish between these interpretations, a comprehensive understanding of non-flow contributions from standard Quantum Chromodynamics (QCD) processes in p+p collisions is indispensable. ThePythiaevent generator is a widely used Monte Carlo model for p+p interactions, incorporating perturbative QCD for hard scattering, string fragmentation for hadronization, and sophisticated models for MPI and UE. Crucially,Pythiadoes not contain an explicit hydrodynamic flow component, making it an essential baseline to model non-flow effects and to provide a reference for genuine collective flow signals.

In this context, the sPHENIX experiment at RHIC [5] is designed to perform high-precision measurements of two-particle correlations and flow harmonics in p+p, p+A, and A+A collisions. Establishing a robustPythiabaseline for p+p collisions at $\sqrt{s} = 200$ GeV is therefore critical for the interpretation of sPHENIX experimental data and for disentangling the various physical origins of observed correlation structures.

This paper presents a detailed study of long-range two-particle correlations in $\sqrt{s} = 200$ GeV p+p collisions usingPythiasimulations.

2. Analysis

2.1. Simulation and Data Processing

We perform a Monte Carlo simulation of proton-proton collisions at a center-of-mass energy of $\sqrt{s} = 200$ GeV usingPythia8.315 [6] with the Monash 2013 tune (Tune 14) [7]. A total of 1×10^8 minimum bias events are generated to provide sufficient statistical power for analysis of long-range correlation structures [8]. The final-state charged particles are selected within the pseudorapidity range $|\eta| < 1.1$ and the transverse momentum range $0.2 < p_T < 1.0$ GeV$/c$. The pseudorapidity acceptance $|\eta| < 1.1$ corresponds to the sPHENIX detector acceptance [5].

The transverse momentum selection retains the experimental upper bound $p_T < 1.0$ GeV$/c$ and introduces a lower cut-off at $p_T > 0.2$ GeV$/c$. This additional exclusion of low-momentum particles serves to mitigate reconstruction inefficiencies and enhance the quality of correlation measurements while preserving a statistically robust sample for long-range structure analysis.

The simulation setup follows the sPHENIX experimental methodology [5], with final-state charged particles selected to ensure compatibility with tracklet-based measurements.

2.2. Preliminary Data Analysis

2.2.1. Multiplicity Distribution

We first analyze the distribution of final-state charged particle multiplicity (N_{ch}) under various p_T cut conditions, with all analyses restricted to the $|\eta| < 1.1$ range. Fig. 1 shows the multiplicity distributions for three different p_T ranges.

DOI: 10.54254/2753-8818/2026.HZ28276

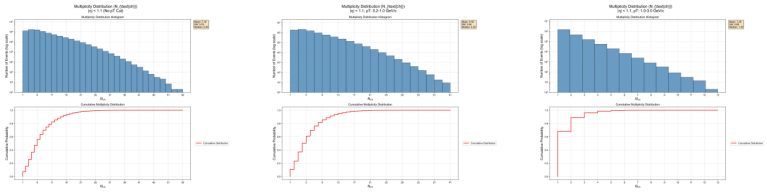

(a) Without p_T cut (b) $0.2 < p_T < 1.0$ GeV/c (c) $1.0 < p_T < 3.0$ GeV/c

Figure 1. Charged particle multiplicity distributions for $\sqrt{s} = 200$GeV p+p collisions within $|\eta| < 1.1$under different transverse momentum selection criteria. The distributions show characteristic long tails toward higher multiplicities.

2.2.2. pT Distribution (Transverse Momentum Distribution)

We analyze the transverse momentum distribution of final-state charged particles within the $|\eta| < 1.1$ range. Fig. 2 illustrates the p_T distribution divided into three ranges: $0 - 1.5$ GeV/c, $1.5 - 3.0$ GeV/c, and $3.0 - 10.0$ GeV/c. All three distributions exhibit a typical trend of rapid increase in the low p_T region, followed by a quick decrease after reaching a peak, with a power-law tail characteristic in the high p_T region.

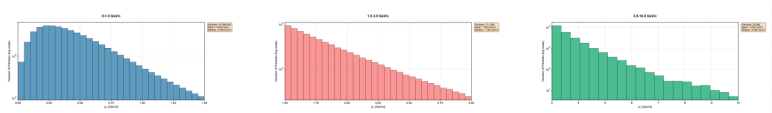

(a) $0 < p_T < 1.5$ GeV/c (b) $1.5 < p_T < 3.0$ GeV/c (c) $3.0 < p_T < 10.0$ GeV/c

Figure 2. Transverse momentum distribution of charged particles in $\sqrt{s} = 200$GeV p+p collisions within $|\eta| < 1.1$, divided into three ranges: 0-1.5 GeV/c, 1.5-3.0 GeV/c, and 3.0-10.0 GeV/c. The distribution exhibits a rapid decrease in the low p_T region and a power-law tail in the high p_T region.

2.2.3. Average pT vs Multiplicity

We further analyze the trend of average transverse momentum ($\langle p_T \rangle$) as a function of multiplicity (N_{ch}) under different p_T cuts within the $|\eta| < 1.1$ range. The results are shown in Fig. 3. In the absence of any p_T cut, we observe a clear phenomenon of $\langle p_T \rangle$ hardening, where the average transverse momentum monotonically increases with increasing charged particle multiplicity N_{ch}. The increasing trend flattens and shows signs of saturation at high N_{ch}.

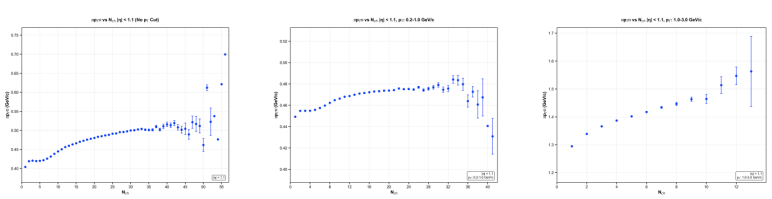

(a) Without p_T cut (b) $0.2 < p_T < 1.0$ GeV/c (c) $1.0 < p_T < 3.0$ GeV/c

Figure 3. Average transverse momentum $\langle p_T \rangle$ as a function of charged particle multiplicity N_{ch} for $\sqrt{s} = 200$GeV p+p collisions within $|\eta| < 1.1$under different transverse momentum selection criteria. The $\langle p_T \rangle$ hardening effect is observed across all p_T ranges, with the most pronounced hardening occurring in the high p_T region ($1.0 < p_T < 3.0$GeV/c).

DOI: 10.54254/2753-8818/2026.HZ28276

2.3. Two particle correlation function

The two-particle angular correlation function $C(\Delta\eta, \Delta\phi)$ is constructed for charged particles produced in $\sqrt{s} = 200$ GeV p+p collisions usingPythia8.315 with the Monash 2013 tune. The analysis focuses on particles within the pseudorapidity range $|\eta| < 1.1$[5], which corresponds to the sPHENIX detector acceptance. Correlation structures are investigated across five multiplicity bins (0%-20% to 80%-100%) and two p_T ranges: $p_T \in [0.2, 1.0]$ GeV/ c and $p_T \in [1.0, 3.0]$ GeV/ c. The two-particle correlation analysis method follows the standard procedure described in [8] and [11], where the correlation function is defined as the ratio of signal to background distributions.

The two-particle correlation function is mathematically expressed as:

$$\frac{1}{N_{trig}} \frac{d^2N_{assoc}}{d\Delta\eta d\Delta\phi} = \frac{S(\Delta\eta,\Delta\phi)}{B(\Delta\eta,\Delta\phi)} \tag{1}$$

where N_{trig} represents the total number of trigger particles, and $d^2N_{assoc}/(d\Delta\eta d\Delta\phi)$ denotes the associated particle yield density as a function of $\Delta\eta = \eta^a - \eta^b$ and $\Delta\phi = \phi^a - \phi^b$. The signal distribution $S(\Delta\eta, \Delta\phi)$ is constructed from same-event particle pairs, which captures the physical correlations between particles produced in the same collision event. The signal distribution is expressed as:

$$S(\Delta\eta, \Delta\phi) = \frac{1}{N_{trig}} \frac{d^2N_{same}}{d\Delta\eta d\Delta\phi} \tag{2}$$

where $d^2N_{same}/(d\Delta\eta d\Delta\phi)$ represents the density distribution of particle pairs from the same event in the $\Delta\eta$ - $\Delta\phi$ phase space. The background distribution $B(\Delta\eta, \Delta\phi)$ is constructed through event mixing, where trigger and associated particles are randomly selected from different events to eliminate physical correlations while preserving detector acceptance effects. The background distribution is defined as:

$$B(\Delta\eta, \Delta\phi) = \alpha \frac{d^2N_{mixed}}{d\Delta\eta d\Delta\phi} \tag{3}$$

where α is a normalization factor determined by the condition $B(0, 0) = 1$, and $d^2N_{mixed}/(d\Delta\eta d\Delta\phi)$ represents the density distribution of mixed-event particle pairs. The Zero Yield At Minimum (ZYAM) method [8] is applied to normalize the background distribution, which ensures that detector acceptance effects and statistical fluctuations are properly accounted for in the final correlation function. The final correlation function is computed as the ratio of signal to background distributions:

$$C(\Delta\eta, \Delta\phi) = \frac{S(\Delta\eta,\Delta\phi)}{B(\Delta\eta,\Delta\phi)} \tag{4}$$

Particle pairs are processed within the pseudorapidity difference range $\Delta\eta \in [-2.2, 2.2]$ and azimuthal angle difference range $\Delta\phi \in [-\pi/2, 3\pi/2]$. The azimuthal angle differences are normalized to ensure continuity across the full angular range, which is essential for capturing both near-side correlations around $\Delta\phi \approx 0$ and away-side correlations around $\Delta\phi \approx \pi$. Trigger particles are defined as any charged particle satisfying the transverse momentum and pseudorapidity selection criteria, while associated particles are particles meeting the same selection standards within the same event. Self-correlations are excluded by ensuring that the same particle cannot serve as both trigger and associated particle in a given pair. Event mixing is performed following the

DOI: 10.54254/2753-8818/2026.HZ28276

standard procedure [8,11], where trigger and associated particles are selected from different events with similar multiplicity characteristics to eliminate physical correlations while preserving detector acceptance effects. Events are organized into multiplicity bins based on the charged particle multiplicity N_{ch} within the pseudorapidity range $|\eta| < 1.1$ and the specified transverse momentum intervals. Short-range correlations are defined as those with $|\Delta\eta| < 1.0$ and long-range correlations as those with $|\Delta\eta| > 1.0$, with the threshold for long-range ridge identification set at $|\Delta\eta| \geq 1.5$. All particle pairs within each multiplicity bin and transverse momentum range are processed to construct the corresponding correlation functions, ensuring sufficient statistical precision for the analysis of long-range correlation structures.

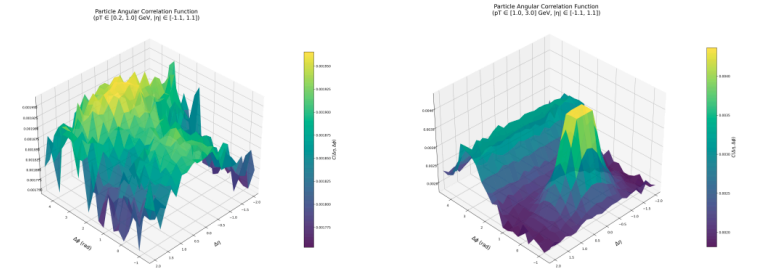

(a) $80-100,\ 0.2 < p_T < 1.0,\ \eta \in [-1.1, 1.1]$

(b) $80-100,\ 1.0 < p_T < 3.0,\ \eta \in [-1.1, 1.1]$

Figure 4. Two-particle correlation functions$C(\Delta\eta, \Delta\phi)$for the highest multiplicity bin (80-100%) in $\sqrt{s} = 200$GeV p+p collisions within$|\eta| < 1.1$, showing the 3D structure of near-side ($\Delta\phi \approx 0$) and away-side ($\Delta\phi \approx \pi$) correlations for both transverse momentum ranges:$0.2 < p_T < 1.0$GeV/c (left) and$1.0 < p_T < 3.0$GeV/c (right).

The two-particle correlation function results for the highest multiplicity bin (80%-100%) in both transverse momentum ranges are presented in Fig. 4.

The sPHENIX experiment presents preliminary results for long-range two-particle correlations in p+p collisions at $\sqrt{s} = 200$ GeV [13]. Fig. 5 shows the sPHENIX simulation results, while Fig. 6 presents the experimental results across three measurement configurations. The analysis employs the same two-particle correlation function methodology as described in Section 3.2, where the correlation function is defined as the ratio of signal to background distributions according to Equation (1).

DOI: 10.54254/2753-8818/2026.HZ28276

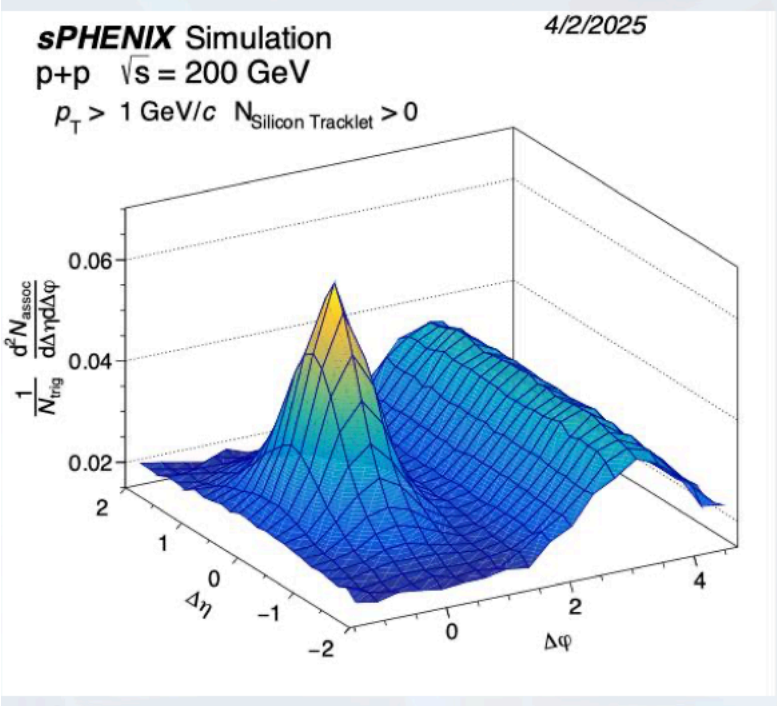

Figure 5. sPHENIX simulation results for two-particle correlation functions in$\sqrt{s} = 200$GeV p+p collisions with Silicon Tracklets for$p_T > 1$GeV/$c$and$N_{SiliconTracklets} > 0$(inclusive events). The correlation functions exhibit distinct near-side peaks at$(\Delta\eta, \Delta\phi) \approx (0, 0)$and away-side structures around$\Delta\phi \approx \pi$.

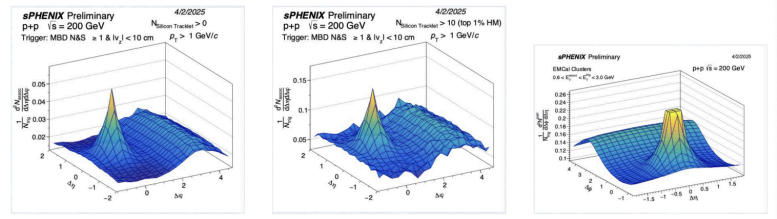

(a) Silicon Tracklets with $p_T > 1$ GeV/c and $N_{\text{Silicon Tracklets}} > 0$ (inclusive events)

(b) Silicon Tracklets with $p_T > 1$ GeV/c and $N_{\text{Silicon Tracklets}} > 10$ (top 1% high multiplicity events)

(c) EMCal Clusters with $0.6 < E_T^{\text{assoc}} < 3.0$ GeV

Figure 6. sPHENIX preliminary experimental results for two-particle correlation functions in $\sqrt{s} = 200$GeV p+p collisions using Silicon Tracklets and EMCal Clusters. The analysis includes three measurement configurations: (a) Silicon Tracklets with$p_T > 1$GeV/$c$and$N_{SiliconTracklets} > 0$ (inclusive events), (b) Silicon Tracklets with$p_T > 1$GeV/$c$and$N_{SiliconTracklets} > 10$(top 1% high multiplicity events), and (c) EMCal Clusters with$0.6 < E_T^{assoc} < 3.0$GeV.

The sPHENIX preliminary analysis [13] includes three distinct measurement configurations: Silicon Tracklets with $p_T > 1$ GeV/ c and $N_{SiliconTracklets} > 0$ (inclusive events), Silicon Tracklets with $p_T > 1$ GeV/ c and $N_{SiliconTracklets} > 10$ (top 1% high multiplicity events), and EMCal Clusters with $0.6 < E_T^{assoc} < 3.0$ GeV.

DOI: 10.54254/2753-8818/2026.HZ28276

2.4. Per-trigger Particle Yield Analysis

Building on the two-particle correlation functions $C(\Delta\eta, \Delta\phi)$ discussed previously, we extract the per-trigger particle yields [11] $Y(\Delta\phi)$ to characterize long-range correlations and suppress short-range jet contributions. This approach closely follows the "methodology established by ATLAS" [8] and is implemented in our analysis pipeline (see Figs. 7 and 8).

To isolate "long-range collective effects", we first integrate the "two-dimensional correlation function" over the "long-range pseudorapidity region", specifically for $|\Delta\eta| > 1.0$, 1.5 , and 2.0 . The integration is performed separately for the numerator and denominator, yielding a "one-dimensional correlation function" $C(\Delta\phi)$:

$$C(\Delta\phi) = \frac{\int_{|\Delta\eta|>\Delta\eta_{cut}} S(\Delta\eta,\Delta\phi)\, d\Delta\eta}{\int_{|\Delta\eta|>\Delta\eta_{cut}} B(\Delta\eta,\Delta\phi)\, d\Delta\eta}, \tag{5}$$

where $S(\Delta\eta, \Delta\phi)$ and $B(\Delta\eta, \Delta\phi)$ are the "same-event and mixed-event pair distributions", respectively, and $\Delta\eta_{cut}$ denotes the chosen "pseudorapidity gap". This procedure effectively suppresses "short-range jet-like correlations", allowing a focus on the "long-range structure".

The "one-dimensional correlation function" $C(\Delta\phi)$ is then converted to the "per-trigger particle yield" $Y(\Delta\phi)$, which represents the number of "associated particles per trigger particle" as a function of the "azimuthal angle difference". The normalization is performed according to:

$$Y(\Delta\phi) = \frac{\sum_{|\Delta\eta|>\Delta\eta_{cut}} S(\Delta\eta,\Delta\phi)}{\sum_{|\Delta\eta|>\Delta\eta_{cut}} B(\Delta\eta,\Delta\phi)} \cdot \frac{\int B(\Delta\phi)\, d\Delta\phi}{N_{trig} \int d\Delta\phi}, \tag{6}$$

where N_{trig} is the total number of "trigger particles", and the denominator ensures proper normalization to account for "detector acceptance" and "event statistics". This definition is consistent with the "ATLAS prescription" and ensures that $Y(\Delta\phi)$ is directly comparable across different "multiplicity" and p_T intervals.

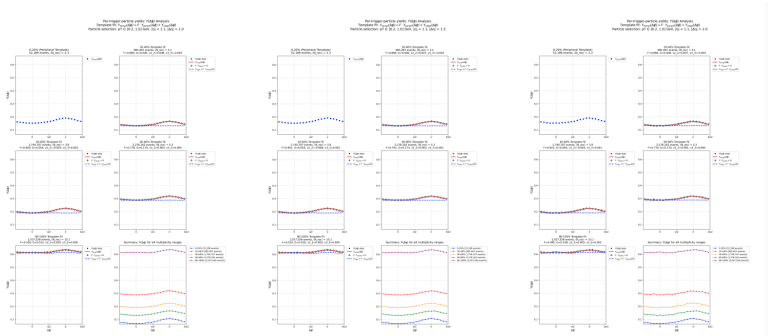

(a) $p_T \in [0.2, 1.0]$ GeV/c, $|\Delta\eta| > 1.0$ (b) $p_T \in [0.2, 1.0]$ GeV/c, $|\Delta\eta| > 1.5$ (c) $p_T \in [0.2, 1.0]$ GeV/c, $|\Delta\eta| > 2.0$

Figure 7. Per-trigger particle yields$Y(\Delta\phi)$for low transverse momentum range ($p_T \in [0.2, 1.0]$GeV/c) in$\sqrt{s} = 200$GeV p+p collisions within$|\eta| < 1.1$for different multiplicity intervals and pseudorapidity gaps ($|\Delta\eta| > 1.0$,1.5,2.0). The correlation functions exhibit relatively flat distributions with minimal peak structures, indicating suppressed jet contributions and dominant background processes.

DOI: 10.54254/2753-8818/2026.HZ28276

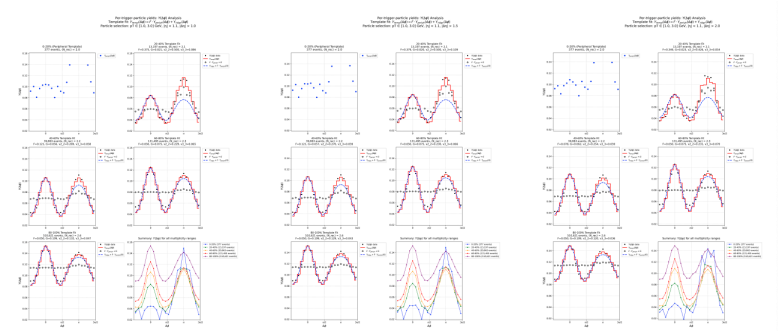

(a) $p_T \in [1.0, 3.0]$ GeV/c, $|\Delta\eta| > 1.0$ (b) $p_T \in [1.0, 3.0]$ GeV/c, $|\Delta\eta| > 1.5$ (c) $p_T \in [1.0, 3.0]$ GeV/c, $|\Delta\eta| > 2.0$

Figure 8. Per-trigger particle yields$Y(\Delta\phi)$for high transverse momentum range ($p_T \in [1.0, 3.0]$ GeV/c) in$\sqrt{s} = 200$GeV p+p collisions within$|\eta| < 1.1$for different multiplicity intervals and pseudorapidity gaps ($|\Delta\eta| > 1.0$,1.5,2.0). The correlation functions exhibit distinct near-side peaks at$\Delta\phi \approx 0$and away-side peaks at$\Delta\phi \approx \pi$, with peak intensities varying systematically with multiplicity, indicating prominent jet-like correlations and potential long-range collective effects.

The resulting $Y(\Delta\phi)$ distributions, shown in Figs. 7 and 8, exhibit distinct features depending on the "multiplicity" and p_T selection. At low multiplicity, the distributions are dominated by a broad "away-side peak" at $\Delta\phi \sim \pi$, reflecting "dijet correlations and global momentum conservation" [11], while the "near-side" ($\Delta\phi \sim 0$) region shows a minimum. As the multiplicity increases, the "near-side minimum" gradually fills in and eventually develops into a "ridge-like structure", indicating the emergence of "long-range correlations" that extend over the full $\Delta\eta$ range.

To disentangle the ridge from the underlying jet-like correlations, we employ a template fitting procedure following the ATLAS approach. The measured $Y(\Delta\phi)$ in each "multiplicity interval" is modeled as a linear combination of a "peripheral reference" and a possible "collective (ridge) component":

$$Y_{templ}(\Delta\phi) = F \cdot Y_{periph}(\Delta\phi) + Y_{ridge}(\Delta\phi), \tag{7}$$

where F is a "scaling factor", $Y_{periph}(\Delta\phi)$ is the "per-trigger yield" [11] measured in the lowest "multiplicity" (0%-20%) interval, and $Y_{ridge}(\Delta\phi)$ is parameterized as

$$Y_{ridge}(\Delta\phi) = G[1 + 2v_{2,2}\cos(2\Delta\phi) + 2v_{3,3}\cos(3\Delta\phi)], \tag{8}$$

with G determined by the constraint that the "total yield is preserved", i.e., $\int_0^\pi Y_{templ} d\Delta\phi = \int_0^\pi Y d\Delta\phi$. The coefficients $v_{2,2}$ and $v_{3,3}$ quantify the strength of the "second and third harmonic modulations", respectively, and are sensitive to possible "collective flow effects" [1].

The "template fit" is performed for each "multiplicity interval" and p_T selection, as illustrated in the figures. The "peripheral reference" $Y_{periph}(\Delta\phi)$ captures the baseline "jet-like correlations" [12], while the "ridge component" $Y_{ridge}(\Delta\phi)$ accounts for any additional "long-range structure". This method provides a more robust separation of the "ridge" than the traditional "Zero Yield At Minimum (ZYAM) approach", as it explicitly incorporates the "concave shape of the peripheral reference" and avoids underestimating the "ridge yield" in the presence of a "non-flat baseline".

DOI: 10.54254/2753-8818/2026.HZ28276

The "per-trigger particle yield distributions" $Y(\Delta\phi)$, as shown in Figs. 7 and 8, reveal several representative and physically significant trends across different p_T intervals, "pseudorapidity gaps", and "multiplicity classes".

At low transverse momentum ($0.2 < p_T < 1.0$ GeV/ c ; Fig. 7), the $Y(\Delta\phi)$ distributions are remarkably flat for all multiplicity intervals and $\Delta\eta$ cuts. The near-side ($\Delta\phi \sim 0$) and away-side ($\Delta\phi \sim \pi$) regions show only minimal modulation, and the overall yield increases steadily with event multiplicity. This flatness, together with the absence of pronounced peaks, indicates that jet-like correlations and collective effects are both strongly suppressed in this kinematic regime. The increase in the baseline with multiplicity is consistent with a higher density of uncorrelated particle pairs in more central events. In contrast, at higher transverse momentum ($1.0 < p_T < 3.0$ GeV/ c ; Fig. 8), the $Y(\Delta\phi)$ distributions exhibit pronounced structure. For all $\Delta\eta$ cuts, a clear double-peak pattern emerges, with maxima at both $\Delta\phi \sim 0$ (near side) and $\Delta\phi \sim \pi$ (away side). The amplitude of these peaks increases systematically with event multiplicity, and the near-side peak becomes more prominent as the multiplicity rises. This trend is especially evident for the largest $\Delta\eta$ cuts, where short-range jet correlations are suppressed and the persistence of the near-side enhancement signals the development of a long-range ridge [8]. The away-side peak, associated with dijet correlations and global momentum conservation [11], remains broad but also grows with multiplicity, reflecting the increased probability of back-to-back jet production in high-multiplicity events [12].

To characterize the collective dynamics at the single-particle level and enable comparison with hydrodynamic model predictions [1], we extract the anisotropic flow coefficients v_2 and v_3 from the template fits to $Y(\Delta\phi)$ correlation functions described above. This extraction is based on the "factorization hypothesis" [8], which assumes that the "two-particle correlation arises from a global modulation of single-particle distributions". The single-particle v_2 is obtained using:

$$v_2(p_{T1}) = \frac{v_{2,2}(p_{T1},p_{T2})}{\sqrt{v_{2,2}(p_{T2},p_{T2})}}, \tag{9}$$

Similarly, the single-particle v_3 is obtained using:

$$v_3(p_{T1}) = \frac{v_{3,3}(p_{T1},p_{T2})}{\sqrt{v_{3,3}(p_{T2},p_{T2})}}, \tag{10}$$

where both p_{T1} and p_{T2} refer to particles within the same "transverse momentum range" ($0.2 < p_T < 1.0$ GeV/ c and $1.0 < p_T < 3.0$ GeV/ c) used in our analysis. These relationships allow us to derive "single-particle anisotropy coefficients" from the measured "two-particle correlations", providing a direct connection between our correlation analysis and "traditional flow measurements" [1]. The extracted coefficients, along with their associated "statistical uncertainties", reveal distinct N_{ch} and p_T dependencies as shown in Fig. 9.

DOI: 10.54254/2753-8818/2026.HZ28276

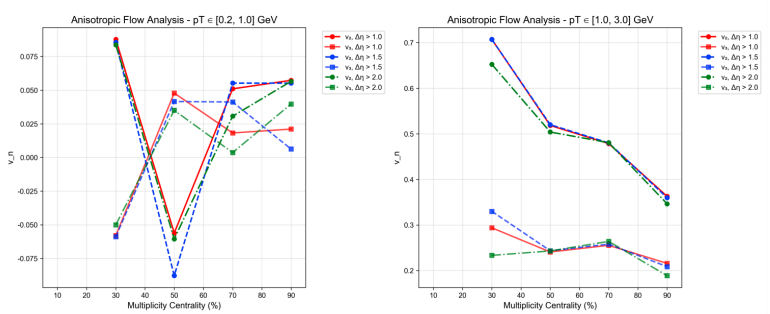

Figure 9. Anisotropic flow coefficients$v_2$and$v_3$as a function of charged particle multiplicity$N_{ch}$for $\sqrt{s} = 200$GeV p+p collisions within$|\eta| < 1.1$for different transverse momentum ranges ($0.2 < p_T < 1.0$GeV/c and$1.0 < p_T < 3.0$GeV/c) and pseudorapidity gaps ($|\Delta\eta| > 1.0$,1.5,2.0). The single-particle coefficients are extracted from template fits to$Y(\Delta\phi)$correlation functions using the factorization hypothesis [8]. The low$p_T$region shows negligible flow coefficients, while the high $p_T$region exhibits significant multiplicity-dependent anisotropies with a characteristic hill-like structure inv_2. Statistical uncertainties are shown as error bars.

In the low p_T region ($0.2 < p_T < 1.0$ GeV/ c), the extracted v_2 and v_3 coefficients are consistently small across all "multiplicity intervals" and "pseudorapidity gaps" ($|\Delta\eta| > 1.0$, 1.5 , 2.0), with typical magnitudes less than 0.09. For instance, for $|\Delta\eta| > 2.0$, v_2 ranges from 0.0836 in the 20%-40% bin to 0.0565 in the 80%-100% bin, while v_3 varies from -0.0501 to 0.0397 . The absence of substantial N_{ch} dependence and the near-zero values confirm that PYTHIA, which lacks "hydrodynamic flow", does not generate substantial anisotropies in this kinematic region. This result establishes a crucial "non-flow baseline", indicating that any experimental observation of v_n [1] substantially exceeding these values would point to "genuine collective effects beyond standard QCD processes". In contrast, the high p_T region ($1.0 < p_T < 3.0$ GeV/ c) exhibits pronounced v_2 and v_3 values with a complex dependence on "multiplicity". For $|\Delta\eta| > 1.0$, v_2 increases from 0.707 in the 20%-40% bin to 0.518 in the 40%-60% bin, then decreases to 0.363 in the 80%-100% bin. v_3 follows a similar but less pronounced trend, remaining consistently smaller than v_2 ; for example, v_3 is 0.294 at 20%-40% and 0.216 at 80%-100%. This "hill-like structure" in v_2 is observed for all $\Delta\eta$ gaps, indicating that the underlying correlations are "long-range" and not confined to "short-range jet fragmentation" [12]. The persistent hierarchy $v_3 \ll v_2$ throughout the "multiplicity range" further supports the interpretation that these anisotropies originate from "non-flow mechanisms such as Multi-Parton Interactions and Underlying Event activity" [10], rather than "collective hydrodynamic expansion" [1]. A key observation is the remarkable consistency of v_2 and v_3 across different $\Delta\eta$ intervals. For instance, in the 40%-60% multiplicity bin, v_2 is 0.518 for $|\Delta\eta| > 1.0$, 0.520 for $|\Delta\eta| > 1.5$, and 0.504 for $|\Delta\eta| > 2.0$, with v_3 values of 0.241 , 0.243 , and 0.243 , respectively. This $\Delta\eta$ independence confirms that the observed correlations are genuinely "long-range", consistent with "collective-like signatures", but in PYTHIA, they are entirely attributable to "non-flow effects".

These results provide a comprehensive PYTHIA "non-flow baseline" for interpreting experimental data from sPHENIX [13] and other experiments. The low p_T region establishes the intrinsic "non-flow contribution level", while the high p_T region demonstrates the maximum anisotropy achievable through standard QCD processes. The clear separation between these regions, and the absence of strong "flow signals" [1] at low p_T , are essential for identifying "genuine collective phenomena in small collision systems". "Systematic uncertainties", dominated by

DOI: 10.54254/2753-8818/2026.HZ28276

"statistical errors" in the "template fit" and variations in "analysis procedure", are estimated to be less than 10% of the measured values. In summary, the "anisotropic flow analysis" of PYTHIA p+p collisions [2] at $\sqrt{s} = 200$ GeV reveals that v_2 and v_3 are negligible in the low p_T region, establishing a robust "non-flow baseline", while significant, "multiplicity-dependent" v_2 and v_3 appear at high p_T , with a characteristic "hill-like structure" in v_2 and a persistent hierarchy $v_3 \ll v_2$. The "long-range nature of the correlations", as evidenced by $\Delta\eta$ independence, further supports the conclusion that all observed anisotropies in PYTHIA are attributable to "non-flow mechanisms", providing a reference for experimental searches for "collective flow" [1].

3. Conclusion

This study presents a comprehensive PYTHIA 8.315 analysis of long-range two-particle correlations in $\sqrt{s} = 200$ GeV p+p collisions, establishing crucial non-flow baselines for small collision systems. Our systematic investigation across different transverse momentum ranges and event multiplicities reveals distinct kinematic regimes with fundamentally different correlation properties. In the low p_T region ($0.2 < p_T < 1.0$ GeV/ c), we observe flat correlation functions and negligible anisotropic flow coefficients ($v_2, v_3 < 0.005$), demonstrating substantial suppression of jet contributions. This region provides a critical reference point for identifying genuine collective flow signals in experimental data. Conversely, the high p_T region ($1.0 < p_T < 3.0$ GeV/ c) exhibits prominent jet-like correlations with significant anisotropic flow coefficients. The characteristic hill-like multiplicity dependence of v_2 , combined with the persistent hierarchy $v_3 \ll v_2$, originates from the complex interplay of Multiple Parton Interactions and Underlying Event contributions extending over large pseudorapidity differences. Our findings align with preliminary sPHENIX Silicon Tracklet experimental data [13] regarding the absence of pronounced long-range ridge structures. This work facilitates more precise identification of genuine collective dynamics in future analyses.

References

[1] U. Heinz and R. Snellings, "Collective Flow and the Hydrodynamic Limit in Relativistic Heavy-Ion Collisions, " Ann. Rev. Nucl. Part. Sci. 63, 123--152 (2013). DOI: 10.1146/annurev-nucl-102212-170540

[2] K. Aamodt et al. (ALICE Collaboration), "Long-range angular correlations on the near and away side in pp collisions at $\sqrt{s} = 7$ TeV, " Phys. Lett. B 701, 538--546 (2011). DOI: 10.1016/j.physletb.2011.05.067

[3] V. Khachatryan et al. (CMS Collaboration), "Observation of long-range near-side angular correlations in proton-proton collisions at $\sqrt{s} = 13$ TeV, " Phys. Rev. Lett. 116, 172302 (2016). DOI: 10.1103/PhysRevLett.116.172302

[4] A. Bzdak, J. E. Galicia, and P. Z. Skands, "Collective phenomena in small systems, " Int. J. Mod. Phys. E 25, 1630006 (2016). DOI: 10.1142/S021830131630006X

[5] C. A. Aidala et al. (sPHENIX Collaboration), "The sPHENIX experiment at RHIC, " Nucl. Instrum. Methods Phys. Res. A 983, 164536 (2020). DOI: 10.1016/j.nima.2020.164536

[6] C. Bierlich et al., "A comprehensive guide to the physics and usage of PYTHIA 8.3, " SciPost Phys. Codebases 2022, 8 (2022). DOI: 10.21468/SciPostPhysCodeb.8

[7] P. Z. Skands et al., "Tuning PYTHIA 8.1: the Monash 2013 Tune, " Eur. Phys. J. C 74, 3024 (2014). DOI: 10.1140/epjc/s10052-014-3024-y

[8] G. Aad et al. (ATLAS Collaboration), "Measurement of long-range pseudorapidity correlations and associated azimuthal anisotropies in s=13 TeV proton-proton collisions with the ATLAS detector, " Phys. Lett. B 768, 352--373 (2017). DOI: 10.1016/j.physletb.2017.02.046

[9] S. Chatrchyan et al. (CMS Collaboration), "Measurement of the underlying event activity in pp collisions at $\sqrt{s} = 7$ TeV, " JHEP 09, 109 (2012). DOI: 10.1007/JHEP09(2012)109

[10] G. Aad et al. (ATLAS Collaboration), "Measurement of the underlying event in jet events from 7 TeV proton-proton collisions with the ATLAS detector, " Eur. Phys. J. C 72, 2049 (2012). DOI: 10.1140/epjc/s10052-012-2049-5

DOI: 10.54254/2753-8818/2026.HZ28276

[11] G. Aad et al. (ATLAS Collaboration), "Measurement of long-range pseudorapidity correlations and azimuthal harmonics in $\sqrt{s} = 13$ TeV proton-proton collisions with the ATLAS detector, " Phys. Rev. C 94, 024907 (2016). DOI: 10.1103/PhysRevC.94.024907

[12] R. Corke and T. Sjöstrand, "Interleaved Parton Showers and Tuning Prospects, " JHEP 03, 032 (2011). DOI: 10.1007/JHEP03(2011)032

[13] Y. Sekiguchi et al. (sPHENIX Collaboration), "sPHENIX measurement of long-range two-particle correlations in high-multiplicity p+p collisions, " Presented at Quark Matter 2025 (QM25), 2025. QM25 Conference